Journal of Sound and Vibration (2002) **257**(5), 887–902
doi:10.1006/jsvi.5066, available online at http://www.idealibrary.com on IDEAL®

THE CALCULATION OF ACTIVELY ABSORBING SILENCERS IN RECTANGULAR DUCTS

JAN J. KRÜGER

J. Eberspächer GmbH & Co., Eberspächerstr. 24, Esslingen 73730, Germany.
E-mail: jan.krueger@eberspaecher.com

(*Received* 15 *January* 2001, *and in final form* 5 *January* 2002)

Active silencers can provide effective solutions especially for the control of low-frequency noise in ducts. To evaluate the performance of this technology in the early design stages it is necessary to predict the insertion loss and adjust the silencer sufficiently precisely to the specific requirements of an application. This paper describes different models for the calculation of actively absorbing wall linings with proportional feedback control applied in splitter silencers as used in rectangular air-conditioning ducts. On the basis of well-established theories for the calculation of passive splitter silencers and a network model of electro-acoustic lumped elements for the wall impedance of each active cassette, it is conceivable to determine their insertion loss. Starting with a rather basic approach, the computational model is refined to increase its modelling accuracy. It is shown that a combination of active wall linings with passive linings yields a high attenuation for a wide frequency band. The theoretical findings compare well with experimental results from a laboratory set-up.

1. INTRODUCTION

Noise control in ducts is a subject of ongoing technical, economical and scientific concern e.g., in applications like air conditioning and exhaust systems of internal combustion engines. While for the mid- and high-frequency range passive silencers fabricated from fibrous or porous material are fairly effective, problems often arise at low frequencies. Here, different kinds of resonators such as expansion chambers and Helmholtz-resonators are applied successfully only for limited bandwidths. The effective frequency range of these resonators can be increased by damping the resonance effect which, however, reduces its noise reduction capability drastically. Therefore, the active control of noise in ducts has long been an area of enormous research effort since it has, especially for low frequencies, the potential for sound attenuation without the restriction to a narrow bandwidth [1, 2]. Numerous scientific and technical papers document the achievements made so far in this particular subject. Some of them are reported in overview articles [3–6].

Active control can be implemented by applying either feedforward or feedback control. Both strategies are utilized for the active control of noise in ducts mostly in the form of single input/single output systems which are especially suitable for the cancellation of one-dimensional wave propagation. Regarding feedforward control, a lot of work has been carried out to design an optimum controller based on suitable software algorithms programmed on fast digital signal processors. The control strategy of these controllers aims at an entire cancellation at the position of the actuator (e.g., loudspeaker). This leads to an entire reflection of the unwanted noise back to the source (upstream) which can

0022-460X/02/$35.00

cause instability of the controller or at least severe loading of the actuator due to duct resonances especially if the duct does not have an anechoic termination [7, 8]. The inherent problem can partly be overcome by arrangements with multiple loudspeakers which emit a unidirectional wave thereby limiting the usable frequency range considerably [9, 10]. Other difficulties arise from the uncertainties of the acoustic transfer functions due to changing conditions during operation which can not only cause performance degradation but also noise amplification and instability. Although often investigated with far simpler controllers, similar problems occur applying feedback control aiming towards the maximum reflection of the incoming wave [11–13]. Apart from that, the inability to predict the performance of the active silencer in the early design stages and consequently the impossibility of providing performance guarantees will ultimately limit the number of applications, at least from the point of view of planners in the construction industry.

Another approach to maximize the noise attenuation of an active silencer arrangement is to absorb the energy of the disturbing wave rather than reflecting it as much as possible. Hereby, the overall insertion loss (IL) is achieved by dissipation along an extended silencer with a certain length and surface or wall area instead of reflection at one particular point in the duct to gain maximum reflection loss (RL). The theory of dissipative silencers is well understood and it shows that a maximum propagation loss (PL) will result from a specific value of the wall impedance Z_w presented by the silencer towards the duct [14–16]. The fibrous or porous materials that are typically used in air-conditioning duct silencers are not suitable to provide this optimum value for Z_w at low frequencies and, consequently, are very ineffective in attenuating low-frequency noise. On the contrary, several small collocated boxes which are each equipped with a microphone, a loudspeaker and a simple proportional feedback controller have the ability to provide suitable wall impedances to achieve a high PL in the low-frequency range. This paper deals with models to calculate these active silencers according to known methods for dissipative passive silencers [17, 18] and show the potential of this technology by some experimental results.

2. MODAL SOUND FIELD IN A RECTANGUALR DUCT

For the calculation of the sound field in a rectangular duct a symmetrical configuration depicted in Figure 1, typical for air-conditioning systems, is considered here. This duct is

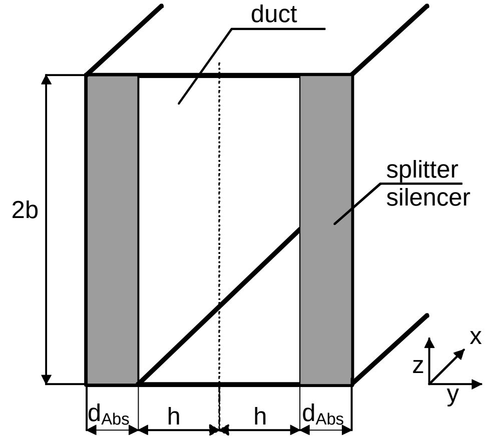

Figure 1. Typical symmetrical configuration of silencers in air-conditioning ducts.

assumed to be rectangular, infinite in length, and the wall lining positioned only on two sides of the duct is locally reacting and also infinitely long. Considering only the symmetrical modes in the duct a pressure distribution in the free duct area can be expressed in the form

$$p(x, y, z) = p_0 \cos(k_y\, y) \cos(k_z\, z)\, \mathrm{e}^{-jk_x x}. \tag{1}$$

The wave number k_y in the y-direction and k_z in the z-direction can be determined by matching the field impedance $Z_0 = \rho_0 c_0$ in the free duct area, to the boundary condition at the silencer surface and the hard duct wall respectively. Inserting equation (1) into the wave equation results in

$$k_x = \sqrt{k_0^2 - k_y^2 - k_z^2}, \tag{2}$$

where k_0 is the free-field wave number in air. Due to the hard wall the particle velocity $v_z = 0$ at $z = 0$ and $z = 2b$. Therefore,

$$k_z = \frac{n_z \pi}{2b} \quad \text{with } n_z = 0, 1, 2 \ldots . \tag{3}$$

For a locally reacting lining there is no sound propagation in x-direction in the silencer material. So, the particle velocity in the y-direction becomes:

$$v_y = \frac{\mathrm{j}}{k_0 Z_0} \frac{\partial p}{\partial y} = \frac{p_0}{Z_W}, \tag{4}$$

where $\mathrm{j} = \sqrt{-1}$, and Z_w is the wall impedance, leading to the defining equation

$$k_y h \tan(k_y h) = \mathrm{j} k_0 h \frac{Z_0}{Z_W} \tag{5}$$

with h being half of the free gap-width in the duct (Figure 1). The propagation loss along the x-axis across the silencer length L_s can now be determined directly from the solution of equation (2) and there especially the imaginary part of k_x:

$$\mathrm{PL} \cong -8{,}68\, L_S\, \mathrm{Im}\{k_x\}\ [\mathrm{dB}]. \tag{6}$$

In such a duct with two walls equally equipped with locally reacting linings, an optimum impedance $Z_{\mathrm{w,opt}}$ exists, which for the two lowest-order modes yields a maximum in the propagation loss per unit length of nearly 19 dB with $L_S = h$ [14–16]. This so-called Cremer-impedance depends only on the density of air ρ_0, the frequency f, and the gap-width h:

$$Z_{\mathrm{W,opt}} = \rho_0 f\, h(1{,}8 - \mathrm{j}1{,}5). \tag{7}$$

It is worth noting, that for usual gap-widths in air-conditioning ducts and under ambient conditions, this optimum impedance and consequently the maximum propagation loss cannot be realized at low frequencies with conventional linings of suitable size containing porous absorber material [17]. Initially, it was the idea of this project to approach the optimum impedance with active silencer cassettes (ASC) in a broad frequency range. Although this aim was clearly missed it will be demonstrated that some remarkable results were achieved at least for the low-frequency range where plane wave propagation dominates.

3. CALCULATION OF THE PROPAGATION LOSS

Actively absorbing silencers as described in references [19, 20] consist of a number of individual cassettes, each containing several electro-acoustic elements, forming a feedback

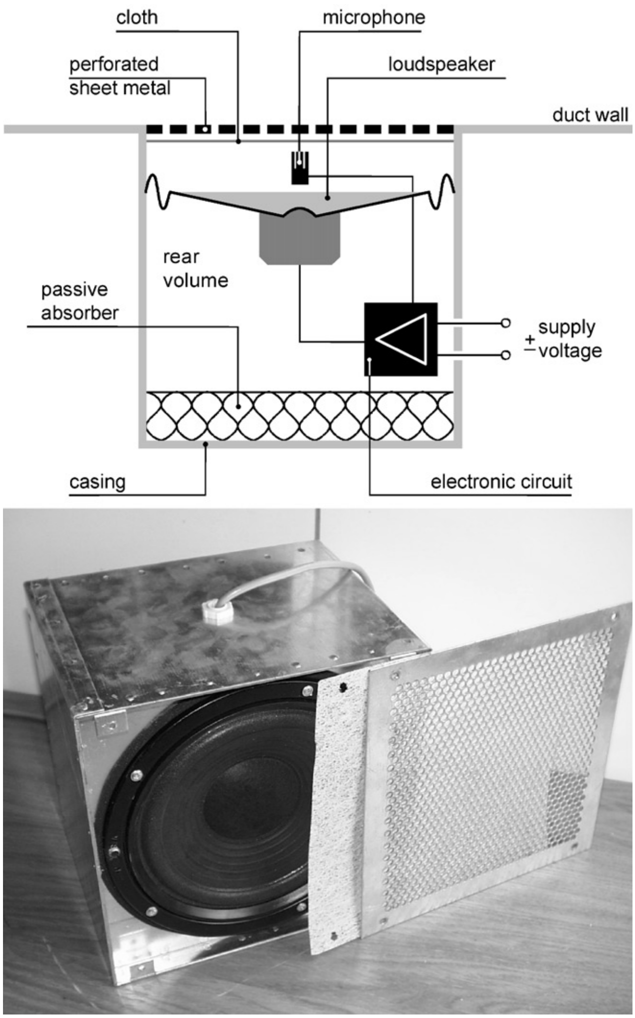

Figure 2. Sketch and picture of an actively absorbing silencer cassette.

loop (Figure 2). The housing of an active silencer cassette (ASC) used in the following investigations has the form of a square box, comprising a standard loudspeaker with a circular membrane at its front area. A more detailed description of the construction and the electro-acoustic network of lumped elements may be found in references [19, 21, 22]. Based on a network model of lumped elements the wall impedance Z_W of each cassette can be determined with sufficient accuracy. A cascaded set of individual ASCs forms the active lining of a rectangular splitter silencer as shown in Figure 3. For the calculation of the wall impedance Z_W of an ASC it has to be considered, that the area of the vibrating loudspeaker membrane A_{Mem} is always smaller than the rectangular overall-area A_W directed towards the inside of the duct. As an approximation, a constant volume velocity is assumed, such that

$$v_{\mathrm{W}} = v_{\mathrm{Mem}} \frac{A_{\mathrm{Mem}}}{A_{\mathrm{W}}}. \tag{8}$$

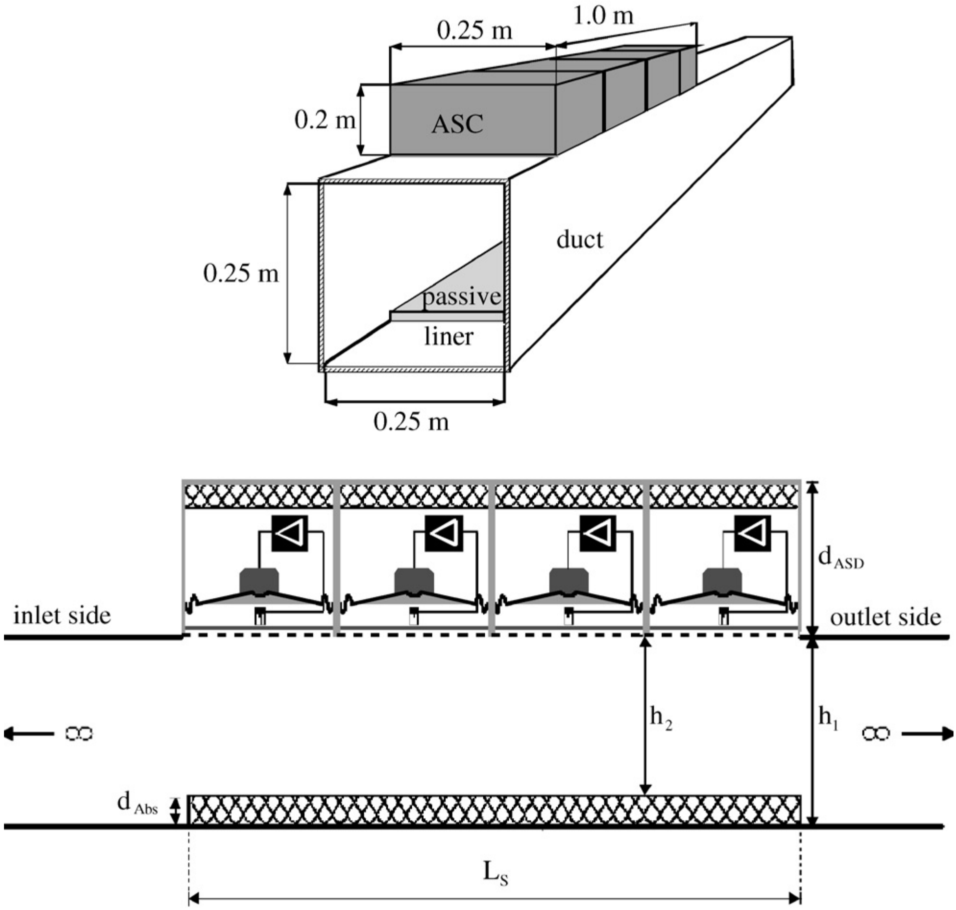

Figure 3. Perspective and side view sketches of an actively absorbing silencer consisting of four cassettes mounted on top of a duct.

Thus, the wall impedance Z_W defined as the ratio of sound pressure p_0 and normal particle velocity v_y is taken as equal or homogeneous over the entire surface area. This way, one also neglects any near field effects, which is strictly valid only up to a frequency where the geometrical dimension are smaller than the wave length but will be used here for simplicity reasons. To investigate the propagation loss of a silencer with an actively absorbing wall lining an arrangement according to Figure 3 is chosen. Here, four ASCs are combined to a silencer of 1 m in length and are attached on top of a duct with a cross-section of $A_K = 0{\cdot}25\,\mathrm{m} \times 0{\cdot}25\,\mathrm{m}$. On the opposite wall there is fixed a layer of porous absorber material with a thickness $d_{Abs} = 40\,\mathrm{mm}$ and a flow resistivity $\Xi_{Abs} = 12\,\mathrm{kPa\,s\,m^{-2}}$ to stabilize the electro-acoustic feedback-loop. Its acoustic impact at low frequencies can be neglected. Nevertheless, since the propagation loss of the arrangement shall be computed in a frequency range from 31 to 2000 Hz it is necessary to consider the propagation loss of the absorber layer at mid- and high-frequencies too. The calculation is consequently carried out in two sequential steps according to the known method for locally reacting silencers. To approximate the solution for k_y of the defining equation (5) the method of continued fractions is employed [15, 17, 18]. This method has proven to yield sufficiently accurate results for realistic sets of parameters (Z_w, Z_0, h) and, moreover, is robust and fast compared to exact algorithms. Consequently, the tangent is replaced by a continued fraction:

$$\tan[(k_y h)^2] = \cfrac{(k_y h)^2}{1 - \cfrac{[(k_y h)^2]^2}{3 - \cfrac{[(k_y h)^2]^2}{5 - \ldots}}} \tag{9}$$

and this development is stopped after the fourth-term leading to the following polynomial equation in $(k_y h)^2$, which is fairly accurate at least around the two lowest duct mode orders:

$$[(k_y h)^2]^4 + c_3[(k_y h)^2]^3 + c_2[(k_y h)^2]^2 + c_1(k_y h)^2 + c_0 = 0. \tag{10}$$

In a further approximation for the calculation of k_x from Z_W of the active and passive lining, the opposite side is neglected, respectively, hence yielding two symmetrical silencers in parallel. This can be justified insofar as for low frequencies the porous absorber layer is acoustically nearly ineffective. Consequently, the virtual gap-width for the active part amounts to about $h_1 = 0{\cdot}25\,\mathrm{m}$ (Figure 3). Furthermore, the surface of the loudspeaker membrane can be regarded as acoustically hard at high frequencies so that for the passive silencer part $h_2 = 0{\cdot}21\,\mathrm{m}$ is valid. The sum of the active (PL_A) and the passive term (PL_P)

$$\mathrm{IL} \sim \mathrm{PL} \sim \mathrm{PL}_A + \mathrm{PL}_P \tag{11}$$

nearly yields the propagation loss (PL) which in this case is almost equal to the insertion loss (IL) of the entire arrangement [23].

The electro-acoustic stability of an ASC is strongly dependent on the electrical feedback gain of its proportional feedback controller which amplifies the microphone voltage and feeds the signal to the voice coil of the loudspeaker. Here, for all four ASC an electrical feedback gain of $G_{1,2,3,4} = 18\,\mathrm{dB}$ was implemented with the aim of a maximum PL. This figure was gained from a numerical stability analysis and could also be realized in the measurements without stability problems [24]. Under these conditions, the wall impedance Z_{WA} of the active lining can be deduced from the network model comprising the data of the loudspeaker, microphone, electrical circuitry as well as all relevant geometrical data [21, 24]. Moreover, the wall impedance of the passive liner Z_{WP} can be derived according to an empirical model from the given material and geometrical data assuming local reaction as well [25].

In this way, the propagation loss of the arrangement of Figure 3 has been calculated with a frequency resolution of 1/120th octave and plotted with 1/12th octave in Figure 4 in comparison to the results of the IL measurement according to the relevant standard [26]. Hereby, it turned out that the contribution k_z for the overall attenuation is negligible in the frequency range of interest. For easier modelling it was therefore set $k_z = 0$ in equation (2) for all further calculations. Because the measurement was carried out with a fixed microphone position in the duct centre, the experimental result is shown only up to a frequency of 1200 Hz due to cut-on of the second transverse duct mode at about 1360 Hz. Measured and calculated insertion loss data depict one major peak of nearly 40 dB at around 110 Hz due to the active lining and a minor peak of 15 dB at around 900 Hz due to the passive lining. Despite all approximations used, the result of the first calculation is in reasonable agreement with the experimental data. Above 315 Hz, the predicted PL falls slightly below the measured values. There is also a remarkable dip at nearly 750 Hz which can be attributed to the negative losses (amplification) caused by the ASCs [27]. Such a negative propagation loss is a sign for active components showing wall impedances with negative real parts. While at this frequency the negative PL_A of the ASCs can be fully

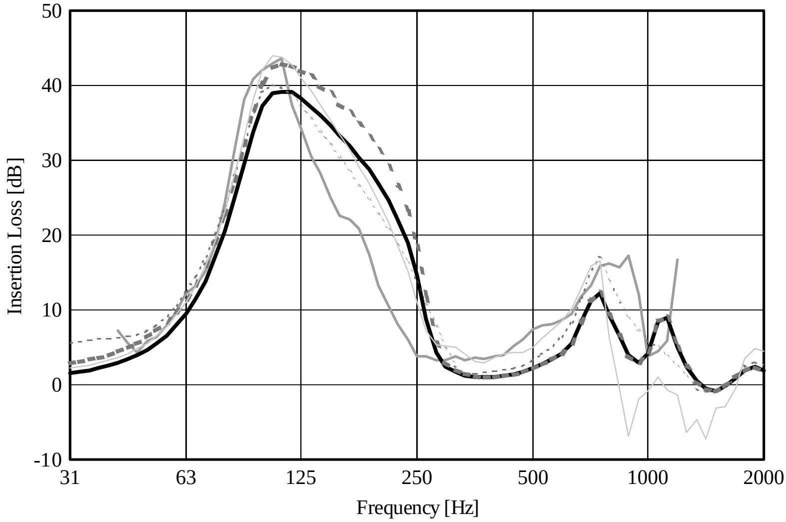

Figure 4. Insertion loss of the actively absorbing silencer according to Figure 3; measured and calculated with equation (11), (12), (17), and on the basis of (19). —— Measurement; ━━ PL1 + PL2; - - - PL1 + PL2 + RL; ······ IL1 + PL2; —— IL asym.

compensated for by the high PL_P of the passive layer this is not the case at about 1500 Hz. Hence, in a limited frequency range noise is amplified rather than reduced by the present arrangement. As pointed out in reference [24], the modelling of the wall impedance of an ASC becomes increasingly inaccurate with rising frequency and varies strongly with frequency from about 800 Hz on.

4. CALCULATION OF THE REFLECTION LOSS

As a result of the sudden change in the wave impedance from Z_0 to Z_x and the wave number k_0 to k_x at the entrance of a silencer and vice versa at the silencer exit, sound waves are reflected. This reflection induces a reflection loss (RL) that in air-conditioning applications can be neglected for most splitter silencers with porous material because it is much smaller than the PL in the frequency range of interest [18, 28]. Nevertheless, since actively absorbing silencers provide a wall impedance with low magnitude especially at low frequencies the influence of the RL on the overall IL must be considered more thoroughly. As a first approach, an approximate addition of all loss components will be computed as usual for dissipative silencers:

$$\mathrm{IL} \sim \mathrm{RL} + \mathrm{PL}_A + \mathrm{PL}_P. \tag{12}$$

Thereby, the reflection loss RL is derived from the transmission coefficient τ or the coefficient of the transfer matrix T respectively,

$$\mathrm{RL} = -10\log\tau = -10\log(|T|^2), \tag{13}$$

where τ depends on the reflection factor R_S of the silencer [19]. Finally, it follows:

$$\mathrm{RL} = -10\log[1 - |R_S|^2] = -10\log\left[1 - \left|\frac{Z_X - Z_0}{Z_X + Z_0}\right|^2\right]\ [\mathrm{dB}]. \tag{14}$$

Both impedance alterations at the entrance and the exit of the silencer are composed of two major parts. On the one hand, for splitter silencers mounted inside the duct there is a reduction of the free duct cross-section by the thickness of the liner d_S and on the other hand, a change in the wave impedance from Z_0 to Z_X due to damping occurs. With the complex wave number k_x in the gap the sought-after wave impedance Z_x becomes:

$$Z_x = \frac{Z_0 k_0 (d_S + h)}{k_x h}. \tag{15}$$

Nonetheless, for the arrangement of Figure 3, the insertion loss is calculated with $d_S = 0{\cdot}0$ m because the silencer is mounted on top of the duct not blocking the free passage of air inside. Furthermore, only the RL of the entrance has to be considered here since it normally exceeds that of the exit [18, 28]. The result of this computation is also shown in Figure 4 and reveals that compared to the prior calculated result there has been a small gain of about 3 dB in the predicted insertion loss only between 80 and 160 Hz, which is in the main operating range of the ASC. This meets the expectations since only in this range the magnitude of the ASCs wall impedance is low compared to Z_0. Altogether, the accuracy of the prediction with a simple inclusion of RL is increased up to 125 Hz, slightly lowered between 125 and 250 Hz and remains nearly unchanged otherwise.

After this first estimation for the RL the transfer-matrix method shall now be used which implicitly incorporates the effect of propagation and reflection loss [29–31]. Hereby, the actively absorbing silencer is regarded as wave-guide of length L_S with internal losses incorporated in a complex wave number k_x. If infinite ducts lengths before and after the silencer are assumed, the transfer matrix which relates the input sound pressure p_{in} and volume velocity q_{in} to the output sound pressure p_{out} and output volume velocity q_{out} becomes:

$$\begin{bmatrix} p_{in} \\ q_{in} \end{bmatrix} = \begin{bmatrix} \cos(k_x L_S) & \mathrm{j} Z_x \sin(k_x L_S) \\ \dfrac{j}{Z_x} \sin\,(k_x L_S) & \cos(k_x L_S) \end{bmatrix} \begin{bmatrix} p_{out} \\ q_{out} \end{bmatrix}. \tag{16}$$

Using equation (13) one can calculate the IL_A of the active liner while the PL_P of the passive liner has to be computed separately and added afterwards since k_x is deduced here only from Z_{WA}. For this reason

$$\mathrm{IL} \sim \mathrm{IL}_A + \mathrm{PL}_P. \tag{17}$$

Figure 4 also includes the result of this computation. Compared to the measurement data both curves exhibit relatively sound agreement up to 1000 Hz. It should be noted, that the difference between all theoretical results shown is only a few decibels at about 100 Hz indicating that the influence of the RL on the IL of this silencer is indeed small. Consequently, most of the sound power in the present set-up is absorbed by the active component as in dissipative silencers rather than reflected as in conventional feedback [10, 12] and especially in feedforward systems [1, 7]. It is assumed, that as in silencers made of porous or fibrous material acoustical power is converted into heat. This process could happen due to friction of air molecules at the cloth next to the perforated sheet metal protecting the cassette, due to mechanical losses within the loudspeaker membrane and its suspension, and due to electrical losses in the resistance of voice coil of the loudspeaker. Nevertheless, the experimental verification of a temperature increase is rather difficult and was not attempted here.

Sometimes, it is of considerable practical importance that the transfer-matrix method also allows a computation in cases where the air-conditioning duct is not infinitely long or terminated as such respectively. Under these circumstances, the attenuation depends strongly on the actual termination, the overall length of the duct, and the position of the silencer in the duct. For example, if the duct is terminated by an opening into a large room, as typical for air-conditioning systems, its low frequency IL is strongly influenced by reflections but this can be accounted for in a careful acoustic design [8, 11].

5. CONSIDERATION OF THE ASYMMETRY IN THE WALL IMPEDANCES

For a more precise calculation of the wave number k_x the asymmetry between the wall impedance Z_{WA} of the actively absorbing lining on one side and the passive layer with Z_{WP} on the opposite side needs to be taken into account (Figure 3). Therefore, it is necessary to superimpose all symmetric and anti-symmetric pressure contributions rather than to add the contributions of two independent symmetrical silencers. While equation (2) remains valid, now, two conditions for Z_{WA} and Z_{WP} have to be fulfilled. The unknown ratio of symmetrical and anti-symmetrical sound pressure can be eliminated by an additional equation for the two different boundary conditions leading to the new defining equation [28, 32] which replaces equation (5):

$$\left[k_y h \tan(k_y h) - \frac{\mathrm{j}k_0 h Z_0}{2}\left(\frac{1}{Z_{Wa}} + \frac{1}{Z_{Wp}}\right)\right] - \left[k_y h \cot(k_y h) + \frac{\mathrm{j}k_0 h Z_0}{2}\left(\frac{1}{Z_{Wa}} + \frac{1}{Z_{Wp}}\right)\right]$$

$$= \left[\frac{\mathrm{j}k_0 h Z_0}{2}\left(\frac{1}{Z_{Wa}} - \frac{1}{Z_{Wp}}\right)\right]^2. \tag{18}$$

Rearranging this expression yields:

$$k_y h - \frac{\mathrm{j}k_0 h Z_0 k_y h}{\tan(2\,k_y h)}\left(\frac{1}{Z_{Wa}} + \frac{1}{Z_{Wp}}\right) + \left[\frac{\mathrm{j}k_0 h Z_0}{2}\left(\frac{1}{Z_{Wa}} + \frac{1}{Z_{Wp}}\right)\right]^2$$

$$- \left[\frac{\mathrm{j}k_0 h Z_0}{2}\left(\frac{1}{Z_{Wa}} - \frac{1}{Z_{Wp}}\right)\right]^2 = 0. \tag{19}$$

The remaining tangent can again be approximated with the method of continued fractions mentioned above in equation (9). The corresponding coefficients for such an expansion up to the fourth order are given in reference [28]. Utilising this algorithm, an effective wave number k_x is deduced for the least attenuated silencer mode and is employed in equation (16) yielding the last theoretical result shown in Figure 4. Sound agreement to the experiment can now be noticed in a frequency range of 250 up to 750 Hz while above this limit even a negative IL is predicted. Since this fortunately does not comply with the measured data it reveals that in this frequency range probably a local reaction of the passive absorber layer cannot be assumed anymore. Instead, a bulk reacting model should be applied which, however, would aggravate the solution of the continued fractioning. The consideration of the silencer as an asymmetrical arrangement is nevertheless an improvement in the important frequency range of low and mid frequencies.

This is especially demonstrated if the asymmetry is enhanced, e.g., by an increasing thickness of the absorber layer to $d_{Abs} = 0{\cdot}1$ m and at the same time a reduction of the gap-width to $h_2 = 0{\cdot}15$ m. With the thickness of the active lining of $d_{ASD} = 0{\cdot}2$ m the width-ratio of $(d_{ASD} + d_{Abs})/h_2$ is equal to 2 which is a value often used in practise. The resulting insertion loss of this modified arrangement is shown in Figure 5. A higher attenuation can be noticed in the whole frequency range. With activated ASCs, the measured as well as the calculated curve shows an IL of more than 20 dB in the range of 80 Hz up to about 800 Hz. Due to the smaller gap-width, the beaming effect which ultimately leads to a reduction of

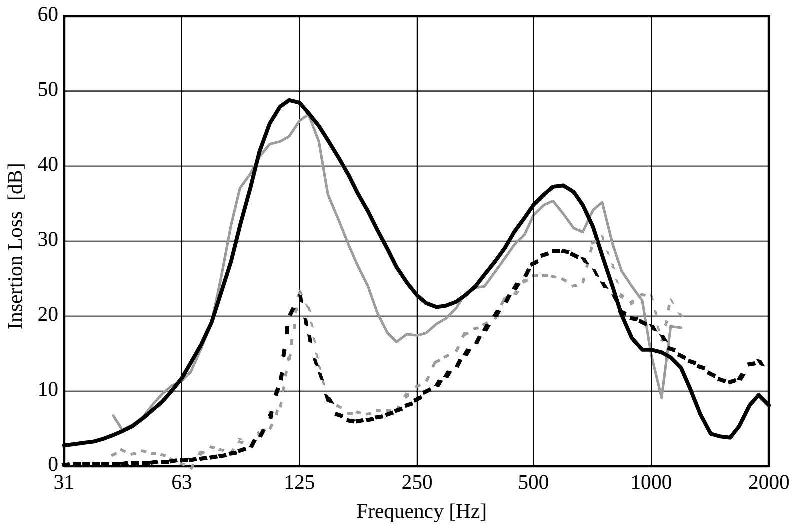

Figure 5. Insertion loss of the actively absorbing silencer according to Figure 3 but with $h_2 = 0{\cdot}15\,\mathrm{m}$; measured and calculated in consideration of its asymmetric lining with the transfer-matrix method according to equation (19); with active cassettes switched on (——) and off (- - - -). —— Measurement with ASC on; —— calculation with ASC on; ······ measurement with ASC off; - - - calculation with ASC off.

IL at high frequencies, starts at nearly 1250 Hz and the loss of attenuation already from about 800 Hz must, therefore, be assigned to the active lining, which is confirmed by the theoretical result.

How much does the active liner contribute to the overall IL result? To answer this question, the feedback loop of all active cassettes was opened (Figure 5). In this case, only the sound pressure inside the duct moves the loudspeaker membranes. Together with the compliant air enclosed in the cassette, they act as passive resonators. This leads to a major IL contribution only near their resonance frequency of about 125 Hz. Elsewhere, the IL is dominated solely by the effect of the passive lining, which can be deduced from the gentle IL-rise from low frequencies to a maximum of about 25 dB at nearly 800 Hz. Comparing the results in Figure 5, one also notes that for the activated ASCs the IL is higher even in the frequency range up to 800 Hz. Thus, the active lining contributes not only in their aimed working range of 50–200 Hz but also up to 800 Hz considerably to the overall IL. The broadband working range of the ASCs thereby spans more than four octaves.

6. INFLUENCE OF THE MICROPHONE POSITION

In all arrangements considered so far, the microphone was located approximately 20 mm above the centre of the cassettes loudspeaker membrane as shown in Figures 2 and 3. This configuration was chosen since for symmetry reasons the sound pressure picked up there by the microphone corresponds best to the averaged sound pressure along the x-axis in the plane of the lining. Also, the behaviour of the active cassettes with an out-of-centre microphone was investigated. Positions near the edge of the cassette are of special practical interest since there the microphone can be implemented easily in the frame of the loudspeaker. If the microphone is mounted in a position on the x-axis shifted towards the sound source one can additionally utilize a possible time lead to compensate for inevitable delays within the signal processing as principally known from feedforward systems [1, 7]. Therefore, the arrangement in Figure 3 was altered by shifting all four

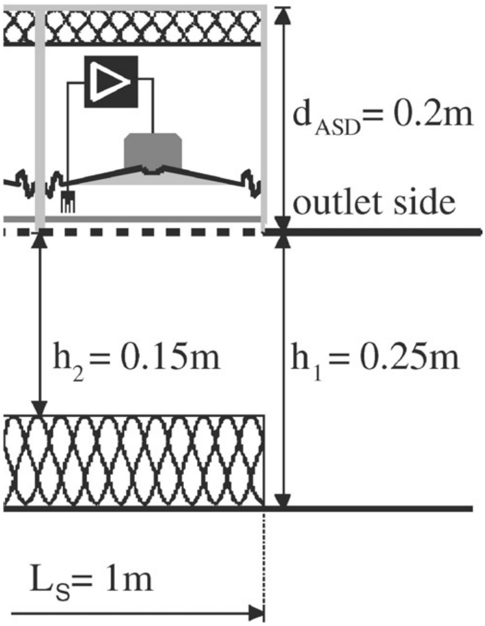

Figure 6. Detail of an actively absorbing silencer similar to Figure 3 but with the microphones shifted towards the inlet side.

microphones 110 mm towards the source (Figure 6). The theoretical modelling of this configuration is less straightforward.

An analytical calculation of the sound field at the edge of a piston for the radiation from a infinite plane into semi-infinite free field was carried out 1958 by Brosze [33]. The approach used there differs from the present case insofar as the surface of a real loudspeaker membrane in the frequency range of interest can be considered neither flat nor rigid. Besides that, the boundary condition of an infinitely rigid plane differs essentially from the practical implementation in a rectangular duct. Under these circumstances, this method does not seem to be applicable for stability calculations as well as IL predictions even for cases with centred microphone. In 1973 Doak thoroughly investigated a configuration with a rectangular piece of the wall vibrating in a hard-walled rectangular duct [34, 35]. As a result, analytical expressions for the sound field depending on the geometrical dimensions and the velocity of the vibrating piece normal to the wall for infinite as well as finite length ducts were presented. These formulas were the basis for a numerical and experimental investigation about the near field of a real loudspeaker in a wall of an air-conditioning duct carried out by Trinder and Nelson [11]. The two cases considered show that even below the first transverse duct mode discrepancies between the calculated and measured results occur in both phase and magnitude of the sound pressure. These discrepancies are even pronounced in small distances to the loudspeaker membrane.

Compared to the above, the present case is more complicated since the membrane is circular, curved, not rigid, there are other non-rigid surfaces next to the cassette, and finally the opposite wall is covered by an absorbing layer. Furthermore, it is necessary to calculate the sound pressure just in the proximity of the membrane up to higher duct modes. It can therefore be assumed that the approaches quoted earlier will not yield more precise results than the used network model despite the remarkable amount of numerical work. To integrate the different microphone position into the network model a simple

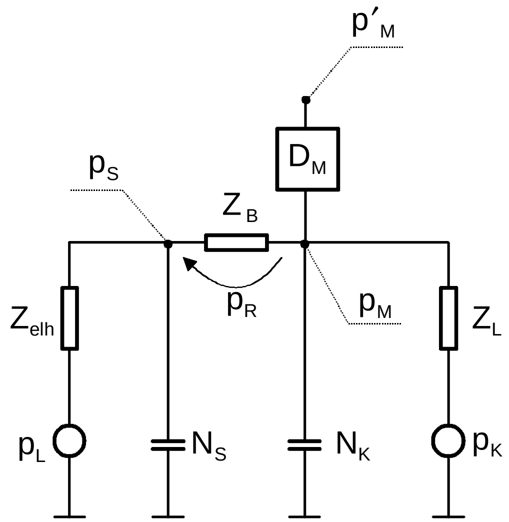

Figure 7. Simplified electro-acoustic network model of an active silencer cassette with the microphone shifted away from the middle of the loudspeaker membrane.

empirical approximation was therefore employed by defining an additional element D_M (Figure 7). This element incorporates the effect of an additional time delay and attenuation across the distance L_M to the centre of the membrane:

$$D_M = \mathrm{e}^{-\Delta L_M (A + \mathrm{j}B)}. \tag{20}$$

The sound pressure p_L generated by the loudspeaker due to the feedback with gain G of the sound pressure at the altered microphone position p'_M then becomes

$$p_L = p'_M G = p_M G D_M = p_M G'. \tag{21}$$

Consequently, the altered sound pressure p'_M can be accounted for by substituting the feedback gain G by G' in the network model described in detail in references [21, 24]. Measurements of the transfer function between the voltage at the terminals of the loudspeaker and the microphone at the frame position showed that the magnitude decreases stronger with rising frequency and the phase shifts more than with the microphone in the centre. However, the stability margins remain nearly unchanged, so that the same linear feedback-gain of $G_{1,2,3,4} = 18\,\mathrm{dB}$ for the controller could be achieved. The comparison of the measurements of the transfer function served to model the coefficients A and B of equation (20). It turned out that with the $A = B = k_0$ the agreement was best in the considered frequency range. Figure 8 shows the IL of the silencer in Figure 6 calculated with G' and its measured result. Again a silencer with a length of $L_S = 1\,\mathrm{m}$, a gap-width $h_2 = 0{\cdot}15\,\mathrm{m}$, and an absorber located opposite ($d_{Abs} = 0{\cdot}1\,\mathrm{m}$; $\Xi_{Abs} = 12\,\mathrm{kPas\,m^{-2}}$) was chosen. Except for the altered microphone position, this arrangement corresponds to the one, with the IL depicted in Figure 5.

The comparison of the curves in Figures 5 and 8 show at first, that especially between 160 and 1000 Hz the IL is increased enormously. The maximum of about 55 dB is close to the limit of the measurable IL for this measurement duct and with the measurement equipment used. Moreover, this means that compared to the results of the deactivated liner which is repeated in Figure 8 an enhancement of up to 25 dB even in the 630 and 800 Hz third-octave bands occurs. If the overall IL is normalized by relating it to the length L_S and the free gap-width h_2 as sometimes used for comparisons of the efficiency of

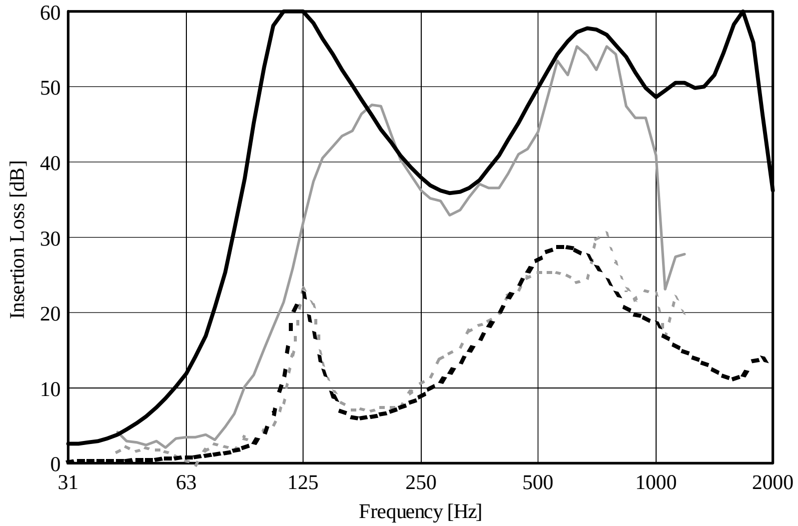

Figure 8. Insertion loss of the actively absorbing silencer according to Figure 6 with $h_2 = 0{\cdot}15\,\mathrm{m}$; measured and calculated in consideration of its asymmetric lining with the transfer-matrix method according to equation (21); with active cassettes switched on (——) and off (- - - -). —— Measurement with ASC on; —— calculation with ASC on; ······· measurement with ASC off; - - - calculation with ASC off.

different dissipative silencers [16, 17]

$$\mathrm{IL}_n = \mathrm{IL}h_2/L_S \tag{22}$$

an IL_n of more than 4 dB over 11 third-octaves can be confirmed (Figure 9). Although far from the optimum value of 19 dB mentioned in section 2, this is indeed a remarkable result for an active silencer of the described geometry. While achieved in combination with a passive liner this result shows that in contrast to common assumptions [3, 5, 6] active silencer technology for air-conditioning ducts can not only be effective at low but also at mid and relatively high frequencies.

The reason for this significant improvement of the IL is seen in the time lead of about 0·3 ms due to the shift of the microphone towards the source. Apparently, this partly compensates some of the inevitable delays in the reaction of the electro-acoustic system, i.e., due to the inert masses involved especially in the frequency range from 160 to 1000 Hz. While the agreement of calculated and measured result between these limits is satisfactory, larger deviations occur at higher and lower frequencies. In both cases, the prediction overestimates the actual result. The uncertainties at very high frequencies must be attributed to the deterioration of the lumped element network model due to increasingly invalid assumptions as explained above. Since the differences at low frequencies do not occur in the case of centred microphone this clearly shows the limitations of the simple approximation with G'. Under the described conditions, an improved modelling seems possible only by employment of numerical methods, such as the finite element and boundary element methods [36]. The additional expenditures for the utilization of these techniques seem however to be justified only in cases where with a deliberate variation of parameters a particular configuration of a silencer has to be optimized and then fabricated in large numbers. Nonetheless, this is much more the case in the field of exhaust silencers for IC-engines rather than for de facto individually planned and tested air-conditioning silencers.

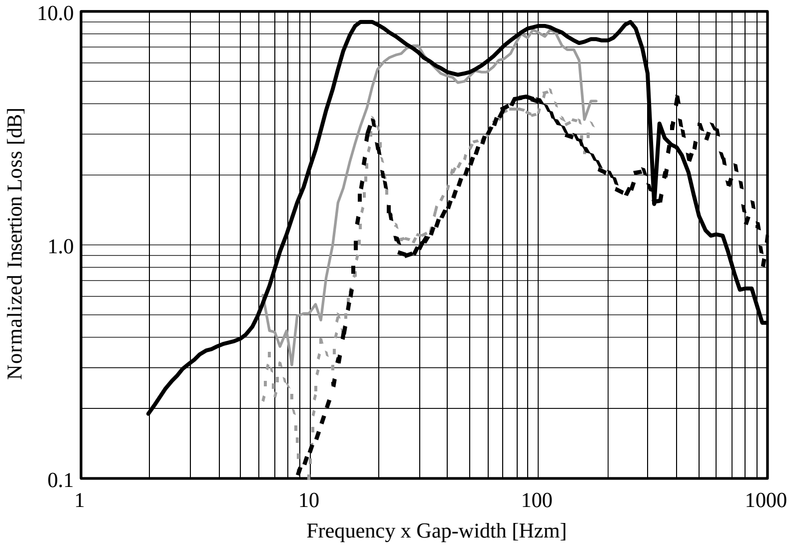

Figure 9. Results of Figure 8 normalised to the ratio of gap-width $h_2 = 0{\cdot}15$ m over length $L_S = 1$ m according to equation (22); with active cassettes switched on (——) and off (- - - -). —— Measurement with ASC on; —— calculation with ASC on; ······· measurement with ASC off; - - - calculation with ASC off.

7. CONCLUSIONS

In the present work, the attenuation of actively absorbing silencers was investigated theoretically and experimentally. Several refined models for the calculation of the insertion loss were developed based on classical passive silencer theory and the wall impedance derived from a network of lumped elements for each independent active cassette. The implementation of an active silencer of 1 m in length consisting of four cassettes in combination with a passive liner on the opposite side led to remarkable IL-results over a broad frequency range demonstrating the effectiveness of this technology. The highest modelling accuracy for the arrangement with the microphone above the centre of the loudspeaker was achieved by utilizing the transfer-matrix method under special consideration of the asymmetry of the lining. Despite the assumptions made, the gained experimental results essentially validated the computational model in the frequency range up to 1000 Hz to an extent, which seems sufficient for the requirements of the IL-prediction in practical air-conditioning design cases.

One of the main findings of this study is that a small shift of the microphone towards the source can significantly improve the IL in the mid-frequency range up to 800 Hz but decreases it in the frequency range below 125 Hz. This was attributed to the compensation of inevitable time delays within the electro-acoustic elements by an earlier detection of the noise signal as principally known by feedforward systems. To incorporate this change of the microphone position in the network model a simple time lead was preferred to analytical and numerical methods. This approximation yielded reasonable accuracy up to about 1000 Hz but failed to predict the decrease of insertion loss below 125 Hz indicating the need for further research efforts. Nevertheless, the final arrangement confirmed, particularly in comparison with the result without activated cassettes, the enormous efficiency even up to frequencies up to 1000 Hz, which is underlined by the high IL$_n$ of more than 2 dB over a broad frequency range of nearly four octaves. Despite the relatively high frequency resolution, all calculations can be carried out on standard personal computers within a few seconds. This assures that in contrast to numerical methods relying on finite elements a quick optimisation for each individual application can be performed in early design stages.

ACKNOWLEDGMENTS

The financial support of the research project "Hybrider Schalldämpfer" carried out at the Fraunhofer-Institute for Building Physics funded by the Volkswagen-Stiftung and the subsequent development project "Reaktiver akustischer Monitor" funded by Ferdinand Schad KG is greatly appreciated. The author would also like to thank the unknown reviewers for their helpful comments as well as Professor Dr. Werner Frommhold for his scientific support throughout the years in Stuttgart.

REFERENCES

1. P. A. Nelson and S. J. Elliott 1992 *Active Control of Sound.* London: Academic Press.
2. L. J. Eriksson 1992 in *Noise and Vibration Control*, Chapter 15 (L. Beranek, editor), New York: John Wiley & Sons. Active Noise Control.
3. J. Tichy 1996 *Noise/News International* **June 4**, 73–86. Applications for active control of sound and vibration.
4. E. F. Berkman and E. K. Bender 1997 *Sound and Vibration* **31**, S. 80–94. Perspectives on active noise and vibration control.
5. L. J. Eriksson 1996 *Noise Control Engineering Journal* **44**, 1–9. Active sound and vibration control: a technology in transition.
6. J. W. Biermann and T. Janowitz 1995 *Lärmminderung im Arbeitsschutz durch Antischall.* Dortmund: Schriftenreihe der Bundesanstalt für Arbeitsschutz.
7. J. Winkler and S. J. Elliott 1995 *Acustica* **81**, 475–488. Adaptive control of broadband sound in ducts using a pair of loudspeakers.
8. J. Krüger, P. Leistner and R. Maute 1998 *Proceedings of EURO-NOISE* 98. *The* 1998 *European Conference on Noise Control,* 1035–1040. Actively absorbing silencers in finite length ducts.
9. M. A. Swinbanks 1973 *Journal of Sound and Vibration* **27**, 411–436. The active control of sound propagation in long ducts.
10. D. Guicking and H. Freienstein 1995 *Proceedings of Active* 95. *The* 1995 *International Symposium on Active Control of Sound and Vibration.* 371–382. Broadband active sound absorption in ducts with thinned loudspeaker arrays.
11. M. C. J. Trinder and P. A. Nelson 1983 *Journal of Sound and Vibration* **89**, 95–105. Active noise control in finite length ducts.
12. W. K. W. Hong, Kh. Eghtesadi and H. G. Leventhall 1987 *Journal of the Acoustical Society of America* **81**, 376–388. The tight-coupled monopole (TCM) and the tight-coupled tandem (TCT) attenuators: theoretical aspects and experimental attenuation in an air duct.
13. T. M. Kostek and M. A. Franchek 2000 *Journal of Sound and Vibration* **237**, 81–100. Hybrid noise control in ducts.
14. L. Cremer 1953 *Acustica* **3**, 249–263. Theorie der Luftschalldämpfung im Rechteckkanal mit schluckender Wand und das sich dabei ergebende höchste Dämpfungsmaß.
15. F. P. Mechel 1991 *Acustica* **73**, 223–239. Modal solutions in rectangular ducts lined with locally reacting absorbers.
16. F. P. Mechel 1998 *Acustica* **84**, 223–244. About the realization of the Cremer admittance of locally reacting duct linings.
17. W. Frommhold and F. P. Mechel 1990 *Journal of Sound and Vibration* **141**, 103–125. Simplified methods to calculate the attenuation of silencers.
18. P. Brandstätt and W. Frommhold and M. J. Fisher 1994 *Applied Acoustics* **43**, 19–38. Program for the computation of absorptive silencers in straight ducts.
19. J. Krüger and P. Leistner 1997 *Proceedings of Active* 97. *The* 1997 *International Symposium on Active Control of Sound and Vibration*, 295–305. Calculation of actively absorbing duct linings.

20. J. KRÜGER and P. LEISTNER 1997 *Applied Acoustics* **51**, 113–120. Noise reduction with actively absorbing silencers.
21. R. LIPPOLD 1995 *Ph.D. Thesis, Technical University of Dresden*. Untersuchung hybrider Absorberkassetten zum Einsatz in Schalldämpferkanälen.
22. S. IRRGANG 1997 *Proceedings of* 1997 *Noise-Con, National Conference on Noise Control Engineering*, U.S.A. 57–70, Design and optimization of active (hybrid) absorbers.
23. J. KRüGER and P. LEISTNER 1996 *INTERNOISE* 25*th INCE Congress*, 1097–1100. Effective noise reduction with hybrid silencers.
24. J. KRÜGER 1999 *Ph.D. Thesis, University of Stuttgart*. Berechnung und praktischer Einsatz aktiv absorbierender Schalldämpfer.
25. M. E. DELANY and E. N. BAZLEY 1970 *Applied Acoustics* **3**, 105–116. Acoustical properties of fibrous absorbent materials.
26. DIN EN ISO 7235: Messungen an Schalldämpfern in Kanälen; 1995–09.
27. J. KRüGER and P. LEISTNER 1998 *Acustica* **84**, 658–667. Wirksamkeit und Stabilität eines neuartigen aktiven Schalldämpfers.
28. W. FROMMHOLD 1991 *Ph.D. Thesis, Technical University of Berlin*. Berechnung rechteckförmiger Schalldämpfer mit periodisch strukturierter Wandauskleidung.
29. M. L. MUNJAL 1987 *Acoustics of Ducts and Muers.* New York: Wiley-Interscience Publication.
30. A. D. PIERCE 1989 *Acoustics—An introduction to its physical principles and applications.* New York: The Acoustical Society of America.
31. P. O. A. L. DAVIS 1996 *Journal of Sound and Vibration* **190**, 677–712. Piston engine intake and exhaust system design.
32. F. P. MECHEL 1976 *Acustica* **34**, 289–305. Explizite Näherungsformeln für die Schalldämpfung in rechteckigen Absorberkanälen.
33. O. BROSZE 1958 *Leitfaden zur Berechnung von Schallvorgängen*. Berlin: Springer-Verlag.
34. P. E. DOAK 1973 *Journal of Sound and Vibration* **31**, 1–72. Excitation, transmission and radiation of sound from source distributions in hard-walled ducts of finite length (I): The effect of duct cross-section geometry and source distribution space–time pattern.
35. P. E. DOAK 1973 *Journal of Sound and Vibration* **31**, 137–174. Excitation, transmission and radiation of sound from source distributions in hard-walled ducts of finite length (II): The effects of duct length.
36. A. CUMMINGS and R. J. ASTLEY 1996 *Journal of Sound and Vibration* **196**, 351–369. Finite element computation of attenuation in bar-silencers and comparison with measured data.